Electronic Supplementary Information

Controlled Fabrication of Hierarchical WO$_3$ Hydrates with Excellent Adsorption Performance

Baixiong Liu[a,b], Jinshu Wang[a,*], Junshu Wu[a], Hongyi Li[a], Zhifei Li[a], Meiling Zhou[a], Tieyong Zuo[a]

[a] College of Materials Science and Engineering, Beijing University of Technology, Beijing 100124, China; [b] Institute of Research and Engineering, Jiangxi University of Science and Technology, Ganzhou Jiangxi 341000,China.

[*] Corresponding author. Tel./Fax: 086-10-67391101. E-mail: wangjsh@bjut.edu.cn (J.S. Wang)

**Table S1.** Pseudo first-order kinetic parameters for the adsorption of MB and Pb^{2+} onto S1 and S2.

MB /Pb^{2+}	C_0 (mg/L)	K_1 (1/min)		$q_{e, exp}$ (mg/g)		$q_{e, cal}$ (mg/g)		R^2	
		S1	S2	S1	S2	S1	S2	S1	S2
MB	100	0.0103	0.0079	99.60	62.20	38.823	44.148	0.8215	0.9147
	80	0.0108	0.0107	79.78	60.32	25.000	26.629	0.7638	0.8615
	60	0.0282	0.0107	59.91	53.02	11.405	19. 828	0.8876	0.8129
	40	0.0198	0.0121	39.96	38.04	2.600	10.343	0.6529	0.7586
	20	0.0220	0.0168	19.99	19.44	1.321	5.395	0.3645	0.4978
Pb^{2+}	70	0.0214	0.0156	69.65	57.05	7.412	12.868	0.6152	0.6446
	60	0.0226	0.0146	59.76	51.18	5.339	8.936	0.6051	0.5345
	50	0.0196	0.0140	49.90	45.25	3.667	6.070	0.4821	0.4398
	40	0.0388	0.0120	40	39.04	1.492	5.595	0.6953	0.3644
	30	0.0372	0.0520	30	30	0.332	6.937	0.2388	0.8044

Table S2. Pseudo second-order kinetic parameters for the adsorption of MB and Pb^{2+} onto S1 and S2.

MB /Pb^{2+}	C_0 (mg/L)	K_2 (g/(mg·min))		$q_{e, exp}$ (mg/g)		$q_{e, cal}$ (mg/g)		R^2	
		S1	S2	S1	S2	S1	S2	S1	S2
MB	100	0.00138	0.00180	99.60	62.20	99.9001	62.7746	0.99884	0.99861
	80	0.00238	0.00234	79.78	60.32	79.9361	60.3865	0.99933	0.99853
	60	0.01286	0.00340	59.91	53.02	60.0936	52.0021	0.99997	0.99896
	40	0.06577	0.00803	39.96	38.04	39.9840	38.0373	1	0.99961
	20	0.29750	0.03486	19.99	19.44	19.9920	19.4401	1	0.99992
Pb^{2+}	70	0.02647	0.00844	69.65	57.05	69.6379	56.9800	0.99997	0.9996
	60	0.03970	0.01265	59.76	51.18	59.7728	51.0465	0.99998	0.9997
	50	0.04579	0.01919	49.90	45.25	49.9002	45.1264	0.99998	0.9998
	40	0.26462	0.01986	40.0	39.04	40.0160	38.8048	1	0.9996
	30	5.55772	0.06905	30.0	30	30.0030	30.0662	1	1

Table S3. Comparison of the adsorption capacities on various adsorbents.

Adsorbents	Adsorption capacity (mg.g^{-1})		Ref.
	MB	Pb^{2+}	
S1	247.3	248.9	This work
S2	117.8	315.0	This work
WO$_3$ nanorods	73.0	–	19
WO$_3$ nanotube	75.0	–	21
Hollow WO$_3$ spheres	138.9	–	26
Magnetite/carbon nanotube	48.1	–	35
Diatomite	156.6	–	37
W$_{18}$O$_{49}$	201	192	38
Attapulgite clay@carbon	–	263.8	39
Hydroxyapatite	–	100	40
Zinc silicate	–	210	41
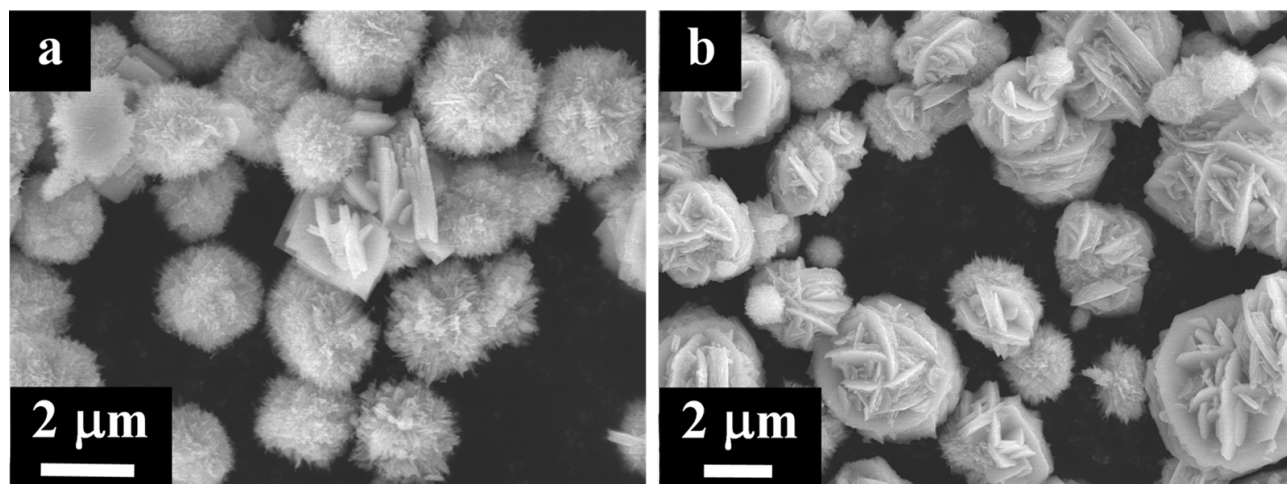
Fig. S1. Typical FESEM images of samples synthesized with different $Na_2WO_4 \cdot 2H_2O$ concentration. (a) 0.02 M,

(b) 0.03 M.
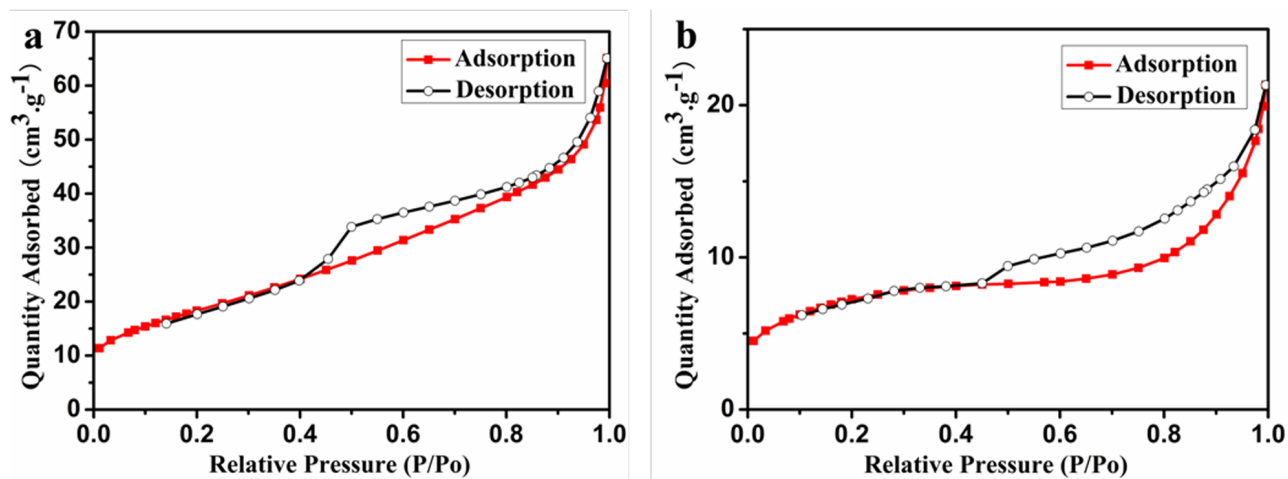
Fig. S2. N_2 adsorption−desorption isotherms of S1 (a) and S2 (b).
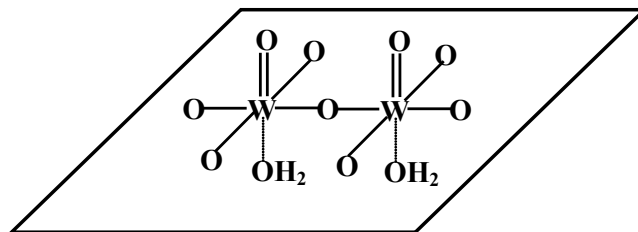
Fig. S3. Schematic illustration of the orthorhombic $WO_3 \cdot H_2O$ structure.

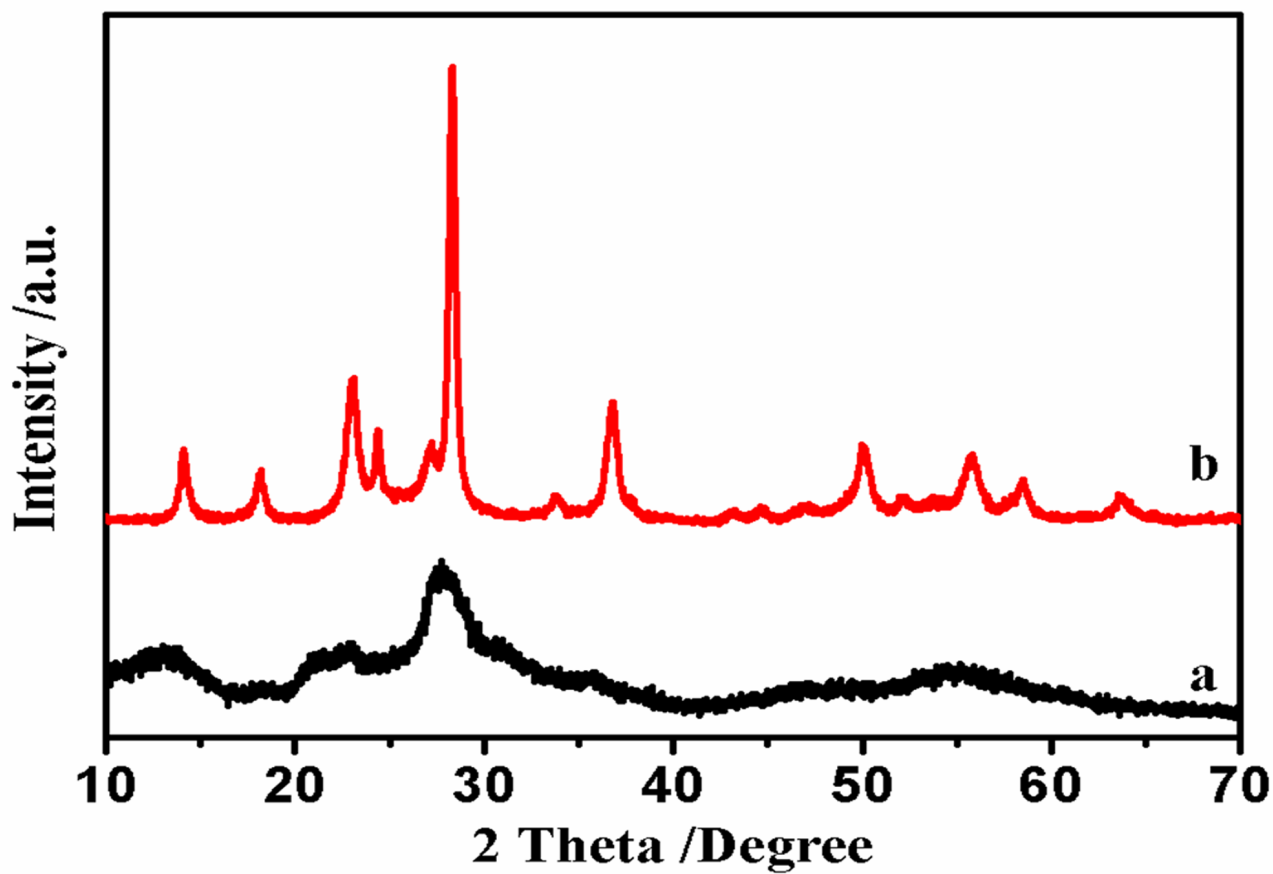**Fig. S4.** XRD pattern of the samples collected at 60 min (a) and 90 min (b).

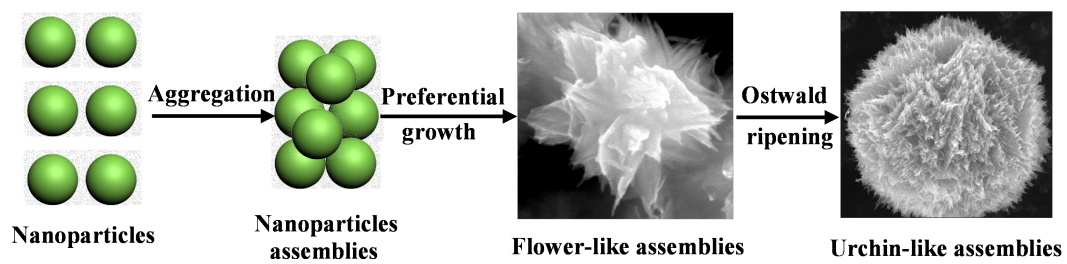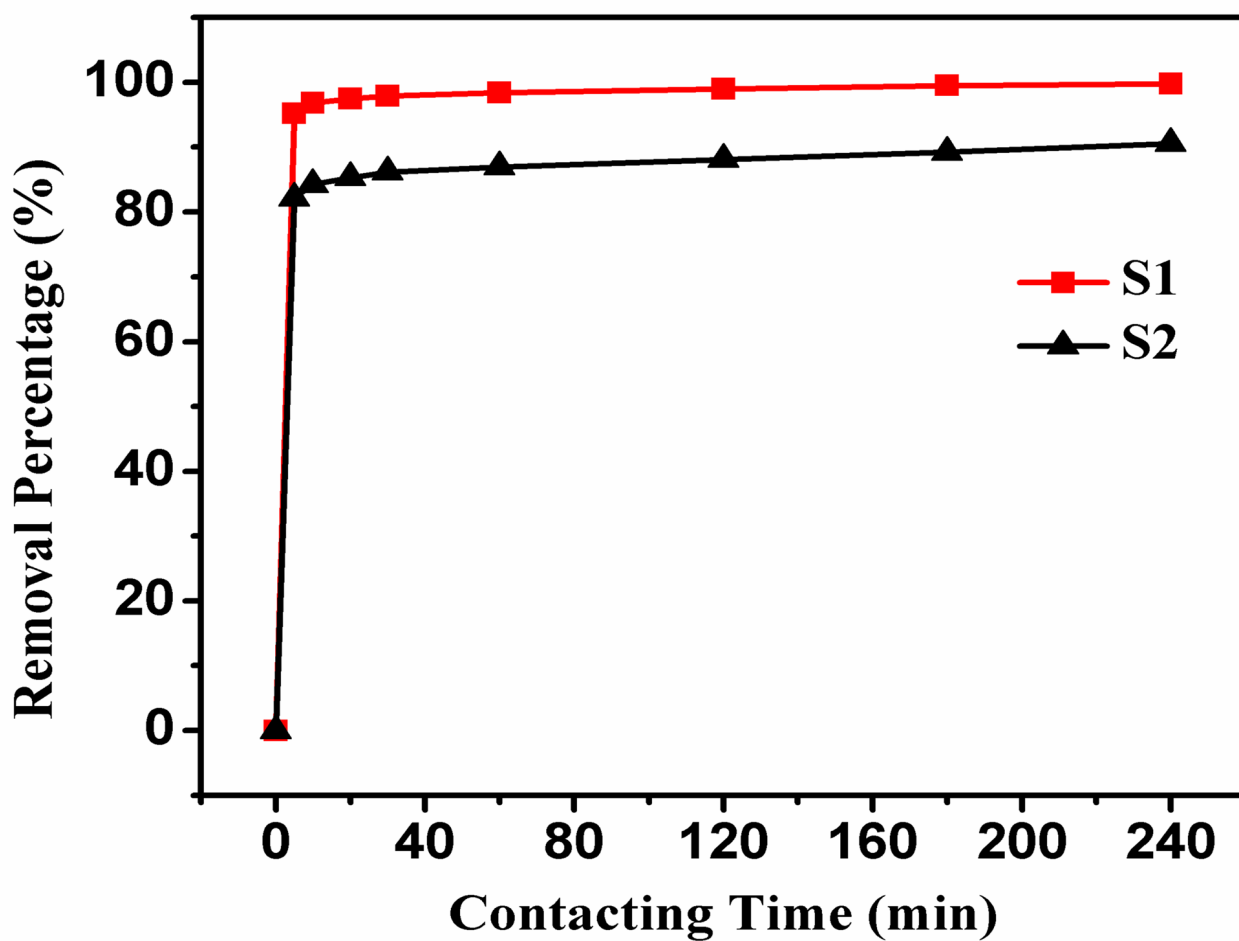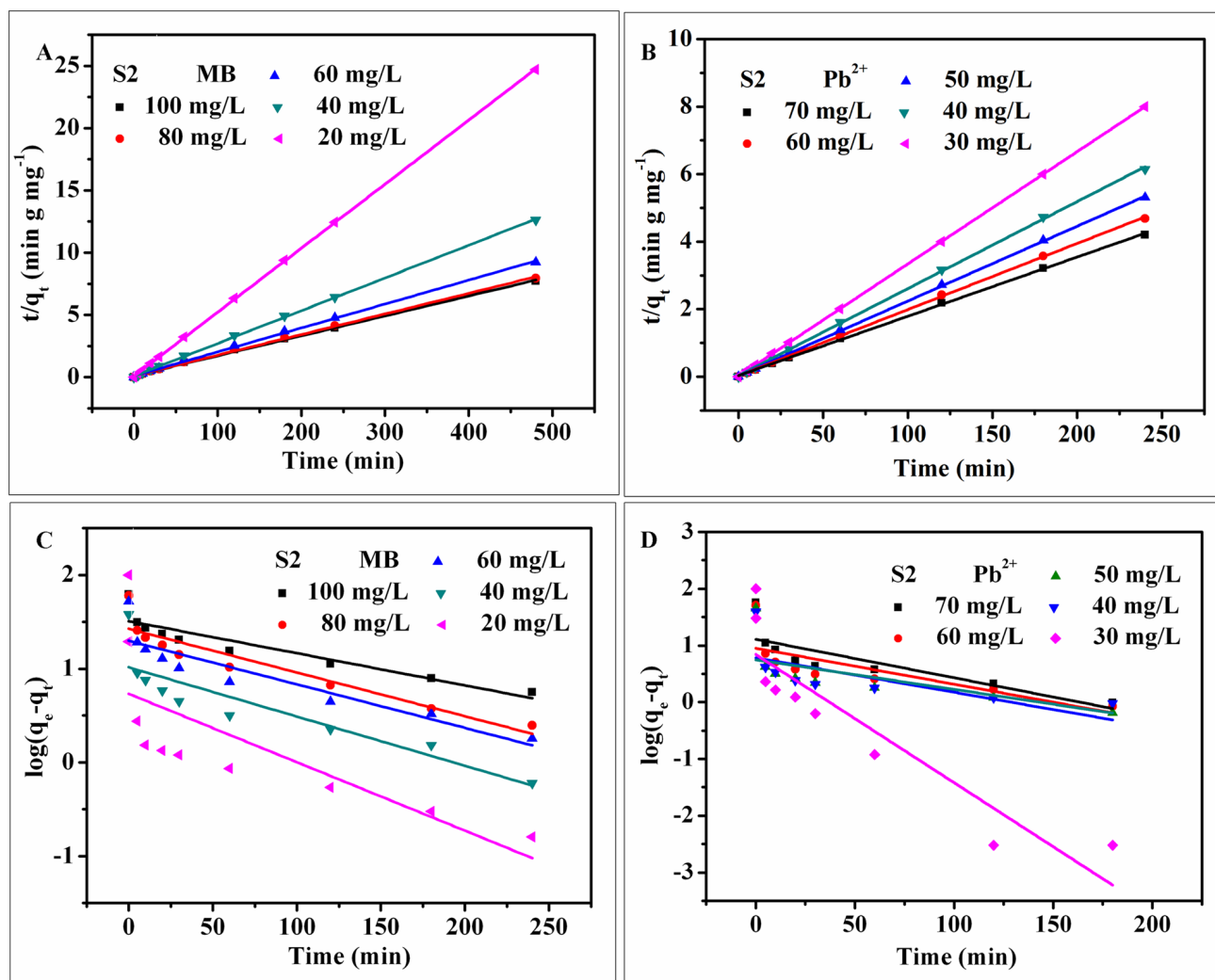**Fig. S5.** Schematic illustration of the formation of S1.

Fig. S6. Adsorption rate curves of Pb^{2+} (initial concentration of 50 mg L^{-1}, 20 mL) in the presence of S1/ S2 (20

mg).

Fig. S7. Pseudo-second-order (A, B) and pseudo-first-order (C, D) kinetic model fitting of the plots for the adsorption of MB and Pb^{2+} onto S2 at different concentrations.
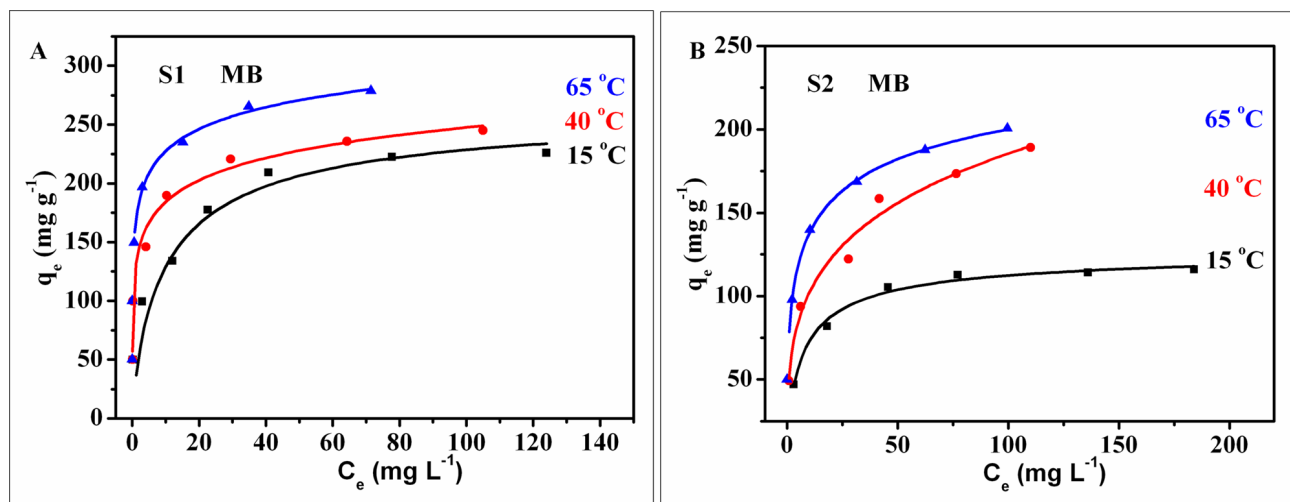
11

Fig. S8. Equilibrium isotherms of MB on S1 (A) and S2 (B) at different temperatures.
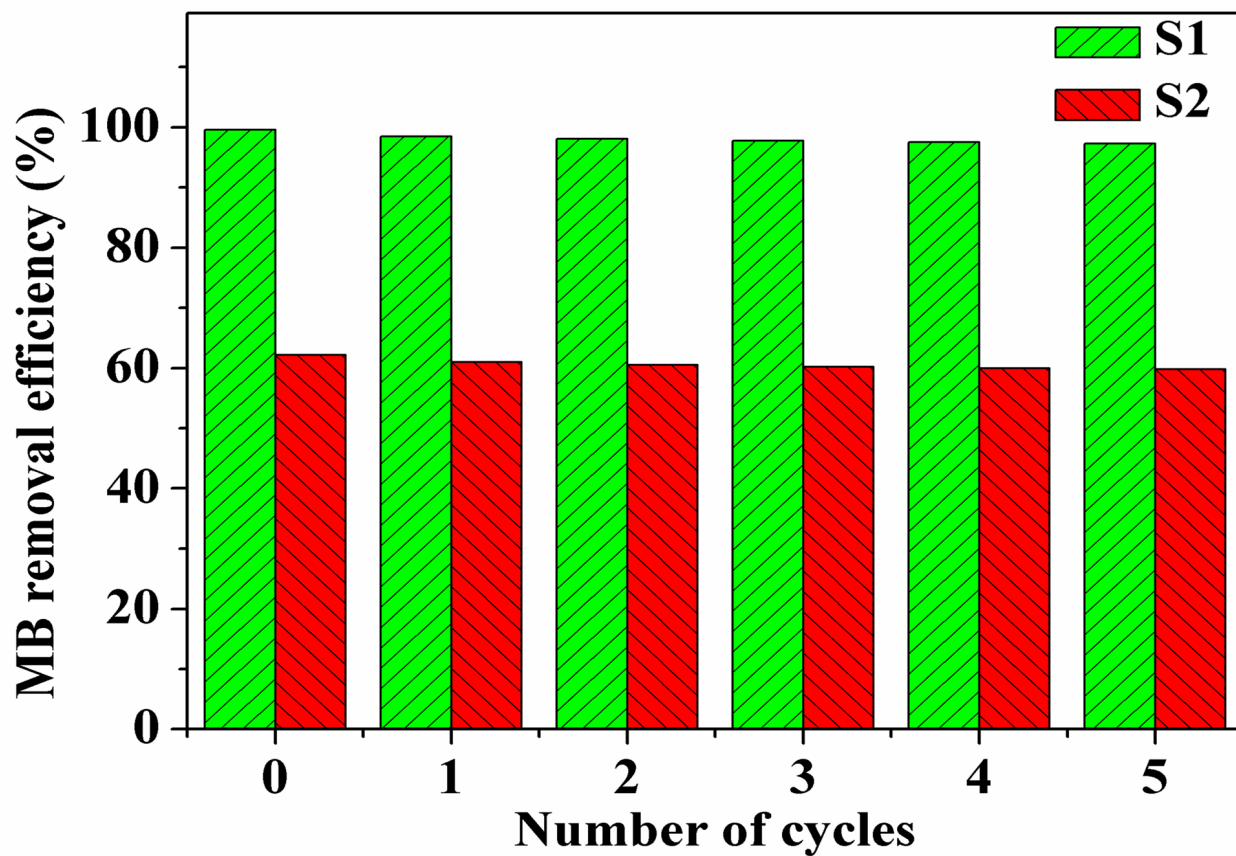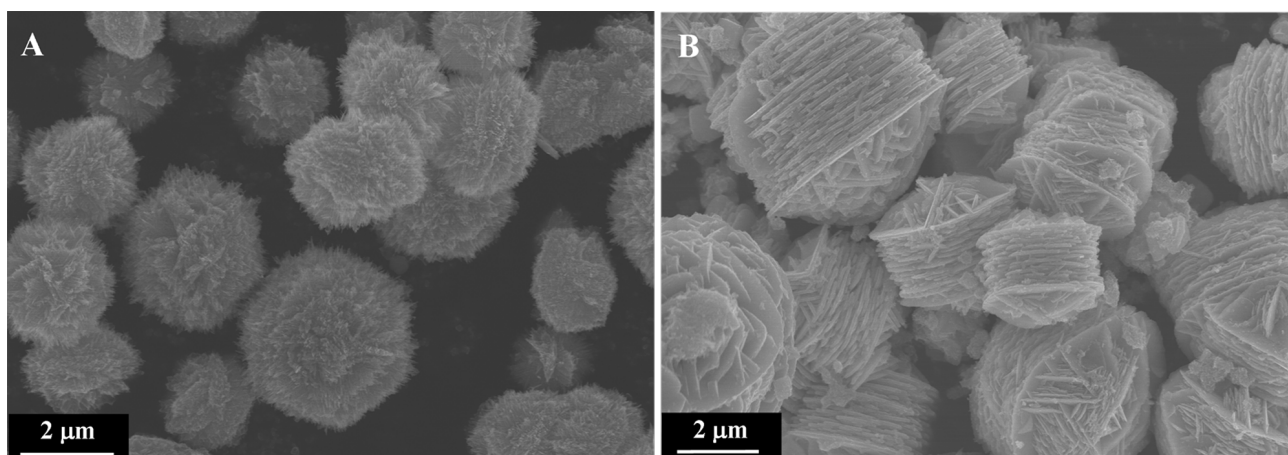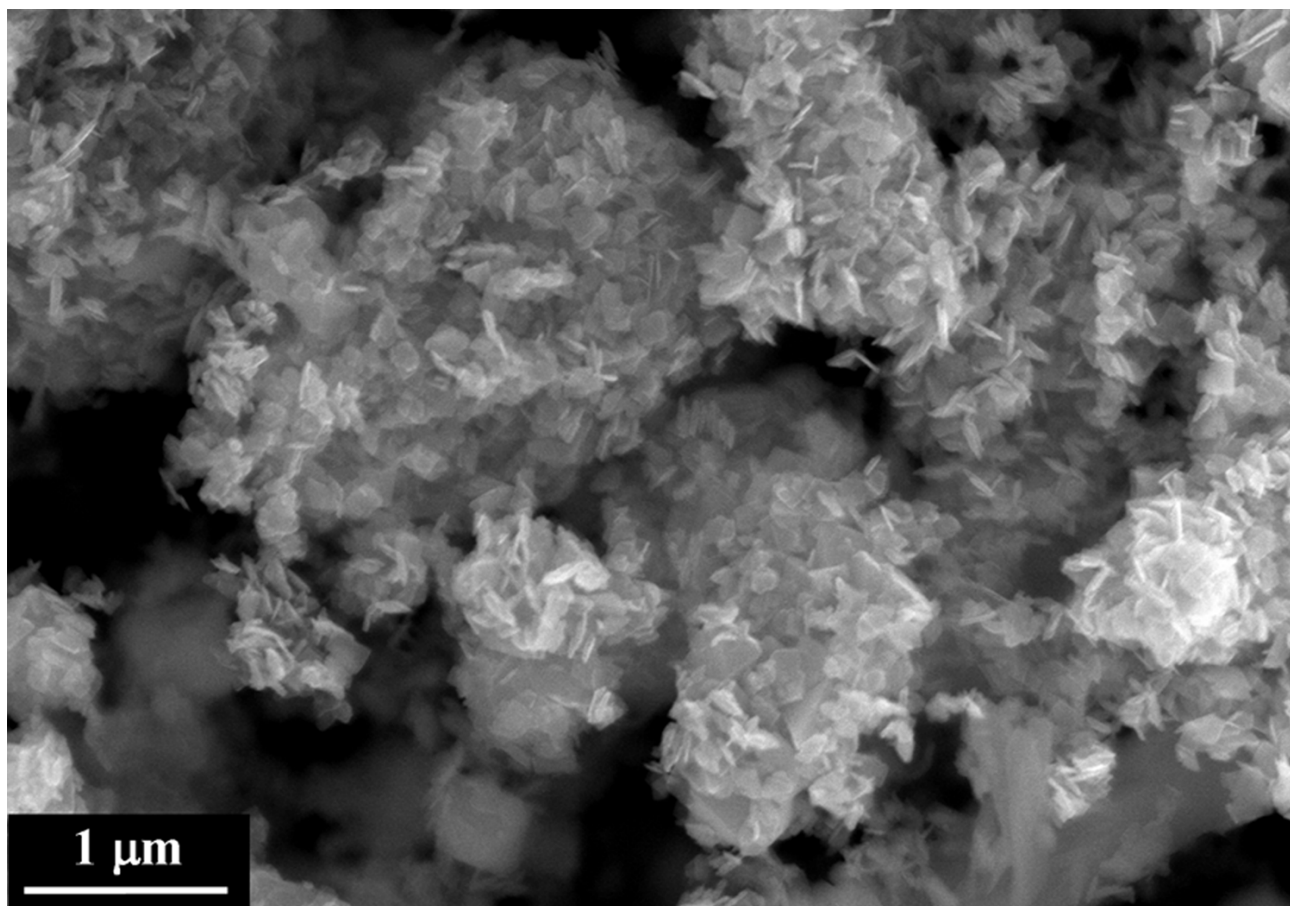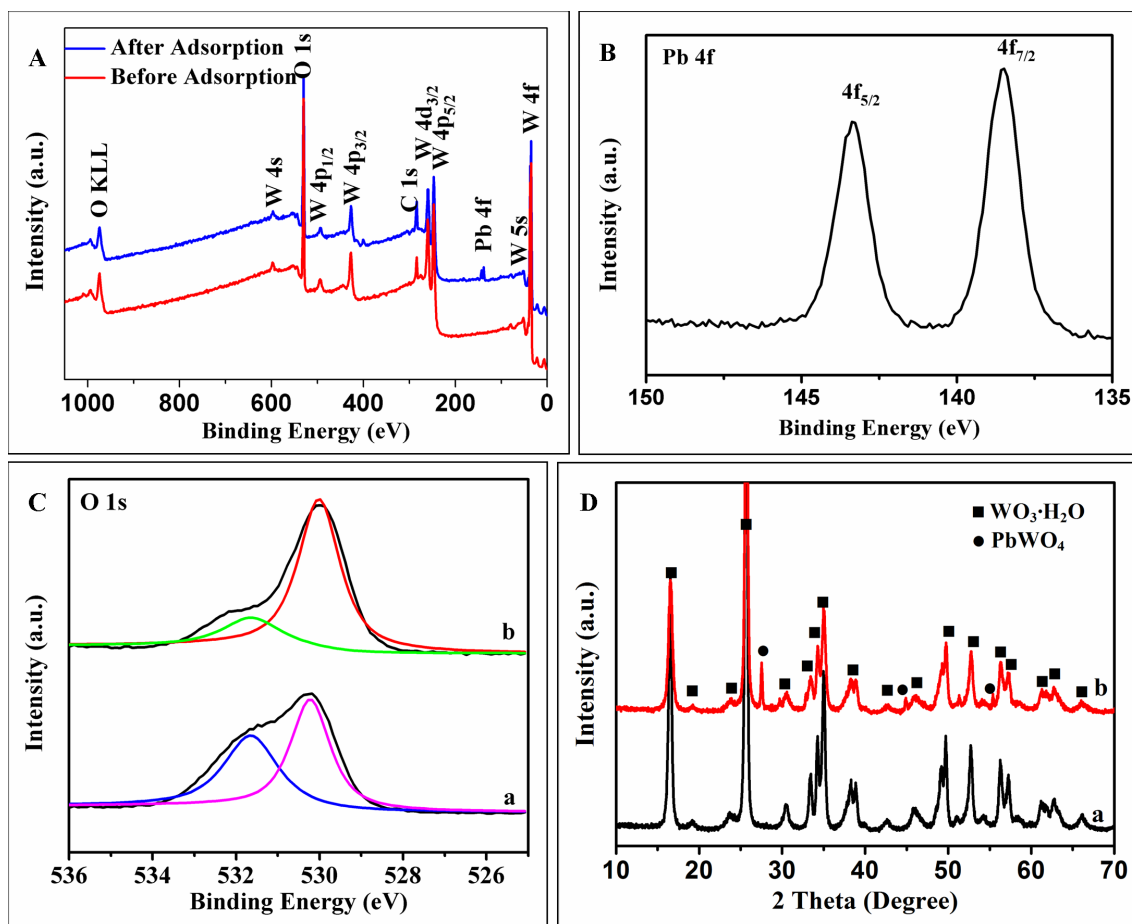
Fig. S9. Adsorption performance of S1 and S2 toward 100 mg/L MB solution within five cycles.

Fig. S10. Typical FESEM images of S1 (A) and S2 (B) after adsorption of MB for five cycles.

Fig. S11. Typical FESEM image of S1 after adsorption of Pb^{2+}.

Fig. S12. (A) Full range XPS spectra of S2 before and after adsorption of Pb^{2+}, (B) XPS spectra of Pb 4f, (C) XPS spectra of O 1s before (a) and after (b) adsorption of Pb^{2+}, (D) XRD patterns of S2 before (a) and after (b) adsorption of Pb^{2+}.

There is also no obvious change in the curves before and after adsorption except for Pb 4f peaks emerging obviously (Fig. S12A). Fig. S12B displays high resolution of Pb 4f peaks after adsorption. Doublet peaks appear at 143.2 eV and 138.3 eV, which are assigned to Pb $4f_{5/2}$ and Pb $4f_{7/2}$, respectively. The peak at 138.3 eV is assigned to the bond of Pb-O, suggesting the formation of lead compound. Fig. S12C shows XPS spectra of O 1s before and after adsorption of Pb^{2+}. A dominant peak at 530.0 eV and a shoulder peak at 531.7 eV are obvious after curve fitting, which is principally attributed to the crystal lattice oxygen (W=O, W−O−W) and surface-adsorbed OH (W−OH), respectively. After adsorption of Pb^{2+}, the peak at 531.7 eV is obviously weakened,

indicating that some of W−OH groups are changed to other groups. The XRD patterns of S2 before (a) and after (b) adsorption of Pb^{2+} are shown in Fig. S12D. After adsorption, all the diffraction peaks can be indexed to $WO_3 \cdot H_2O$ (JCPDS card No. 430679) and $PbWO_4$ (JCPDS card No. 160516), suggesting $WO_3 \cdot H_2O$ have been partially reacted with Pb^{2+}. The results verify the proposed uptake mechanism of Pb^{2+}, and it is also totally accordance with the results shown in Fig. 10.